Journal of Applied Polymer Science

Thermal Stability and Kinetics of Thermal Degradation of PMVS/SiO_2/GO-C_{12}-hep Composites

Huating Qiu, Chengai He, Lianjie Zhou, Hongyun Shao, Hongjie Fan, Hong Mo, Jun Zhang, Ninglin Zhou, Jian Shen

Jiangsu Engineering Research Center for Biomedical Function Materials, College of Chemistry & Materials science, Nanjing Normal University, Nanjing 210023, People's Republic of China

Correspondence to: J. Zhang (E-mail: zhangjun3@njnu.edu.cn) or N. Zhou (E-mail: zhouninglin@njnu.edu.cn)

ABSTRACT: In this study, a series of the PMVS/SiO2/GO-C12-hep (polymethylvinyl siloxane, PMVS) nanocomposites of varying fillers concentration were fabricated employing blending technique. Retained tensile tests showed that tensile strength of PMVS/SiO2/GO-C12-hep nanocomposites improved with increasing of GO-C12-hep content from 0 to 0.5 wt %, but it decreased when the GO-C12-hep content was up to 0.8 wt %. SEM results showed that GO/C12-hep had been dispersed into PMVS matrix, and the interfacial consistency property was very well between GO-C12-hep and PMVS. The degradation mechanism was also analyzed. The thermal stability and the degradation kinetics of nanocomposites had been evaluated using thermo-gravimetric analysis (TGA) at different heating rates in flowing nitrogen. TGA curves revealed that PMVS/SiO2/GO-C12-hep exhibited relatively better thermal stability than PMVS/SiO2, and the degradation temperatures of PMVS/SiO2/GO-C12-hep increased with GO-C12-hep increase. The apparent activation energies (Ea) were estimated with the Flynn–Wall–Ozawa method (FWO method). The Ea of PMVS/SiO2/GO-C12-hep nanocomposites had relevance to their content of GO-C12-hep. © 2013 Wiley Periodicals, Inc. J. Appl. Polym. Sci. 130: 535–542, 2013

KEYWORDS: degradation; copolymers; kinetics

Received 12 November 2012; accepted 9 February 2013; published online 20 March 2013
DOI: 10.1002/app.39165

INTRODUCTION

Silicone rubber has excellent performances for biomedical applications, such as biocompatibility, oxidation resistance, flexibility, air permeability, and biological aging resistance.[1–4] However, many studies have shown that the silicone rubber could lead to blood clots and other adverse consequences when it contacts blood.[5,6] Therefore, silicone rubber must be physically or chemically modified to improve its blood compatibility, when it was used as a blood-contact material.[7–9]

The organic matrix/layered inorganic filler composites have significant advantages when compared with other organic matrix/inorganic filler composites.[10–12] Graphite is a typical layered compound, and the graphite oxide (GO) has been extensively studied as a composite application for its excellent biocompatibility.[13–18] GO is more reactive than pure graphite, which contains —OH and —COOH functional groups as a result of carbon oxidation reactions. Additionally, the distances between GO layers are longer than those of pure graphite. Hence, other molecules can be easily intercalated into GO.

Heparin is a potent anticoagulant which is widely used to prevent and treat thrombosis. Due to its excellent anti-thrombogenic function, heparin is used in many polymeric biomaterials through either physical absorption or chemical binding.[19,20] Some papers have reported that heparin in polymeric biomaterials could substantially reduce the thrombogenicity.[21,22] Benzalkonium chloride (C_{12}) is an antimicrobial agent that has been used in the antimicrobial field.[23]

In our previous study, we had synthesized GO-heparin-C_{12} nanocomposites by interlayer solution, and its antithrombogenic/antibacterial functions and structural characteristics were investigated.[24] The results showed that GO-heparin-C_{12} had not only blood compatibility but also antibacterial function.

In this study, we prepared polymethylvinyl siloxane (PMVS)/SiO_2/GO-C_{12}-hep nanocomposite by mixing PMVS/SiO_2 and GO-C_{12}-hep with a Haake torque rheometer. We attempted to investigate the thermal degradation kinetics of PMVS/SiO_2/GO-C_{12}-hep nanocomposites and its mechanism. And the thermal property of PMVS/SiO_2 as a function of the GO-C_{12}-hep content was examined by way of the activation energy determined from the weight loss during the thermo-gravimetric analysis (TGA).

Table I. The Tensile Properties of PMVS/SiO_2/GO-$C1_2$-hep Nanocomposites with Different GO-$C1_2$-hep Content

Sample	GO-C12-hep content (wt %)	Tensile strength (MPa)	Elongation (%)	Modulus (MPa)
PMVS/SiO_2/GO-C12-hep	0	4.542 ± 0.420	850.637 ± 32.356	0.712 ± 0.023
	0.2	5.526 ± 0.479	950.667 ± 39.400	0.823 ± 0.022
	0.5	5.628 ± 0.243	980.500 ± 30.348	0.776 ± 0.008
	0.8	5.313 ± 0.372	915.449 ± 36.112	0.707 ± 0.054

EXPERIMENTAL

Materials

GO was obtained from Shanghai Chemical Reagent (Shanghai, China). Benzalkonium chloride (C_{12}) and heparin were provided by Sigma (St. Louis, MO). PMVS/SiO_2 was provided by Dongjue silicone (Nanjing, China). Di-2, 4-dichlorobenzoyl peroxide was provided by Mingye Science and Technology Development (Wuhan, China).

Preparation of GO-C_{12}-hep Composite

About 0.4 g of C_{12} was dissolved in 50 mL of distilled water. Heparin (0.4 g) was added into the above solution under stirring condition for 1 h. A white suspension was obtained and used in the latter steps.

About 0.5 g of GO was added in 100 mL 0.1*M* NaOH solution and sonicated for 30 min. C_{12} (0.5 g) was then subsequently added to react with GO under sonication for 15 min. Final precipitation was collected and washed until no chlorine ions were detected. The collection of GO-C_{12} was dried in vacuum oven for 12 h. The above procedure was repeated for preparation of GO-C_{12}-hep.

Preparation of Nanocomposites PMVS/SiO_2/GO-C_{12}-hep

Firstly, PMVS/SiO_2 and an amount of GO-C_{12}-hep were mixed for 30 min at 100°C and 80 rpm in a Haake torque rheometer (Polylab 600), which was provided by Thermo Fisher Scientific (Waltham, MA). Then, the blending and 1.2 wt % Di-2, 4-dichlorobenzoyl peroxide was mixed for 30 min in an open mill, which was provided by Guangyue Rubber Machinery Manufacturing (Qingdao, China). Lastly, the nanocomposites were vulcanized. The premature cure was preformed at 120°C for 10 min and the post cure was performed at 150°C for 2 h.

Tensile Measurement

The tensile tests were carried out at the room temperature using an Instron 4466 tensile test machine (Instron, High Wycombe, UK). The test speed was 200 mm/min. All measurements were carried out five times.

The tensile fracture of samples was observed on JSM-5610 SEM (JEOL Co., Japan). The operation voltage was 20 kV.

ATR-FTIR Measurement

The total reflection fourier transform infrared spectroscopy (ATR-FTIR) spectra were recorded by a FTIR Nexus670 (Nicolet) spectrometer, with a spectral resolution of 4 cm^{-1}. A total of scans were recorded over 4000–400 cm^{-1} for each spectrum.

TGA Measurement

TGA of the samples was carried out on a Pyres 1 TGA (Perkin-Elmer Inc., Wellesleg, MA). All the samples were heated from room temperature to 800°C at a rate of 20°C/min under nitrogen atmosphere to measure the thermal decomposition temperature of nanocomposites.

All samples were heated from room temperature to 600°C at the rates of 5, 10, 20, 40°C/min under nitrogen atmosphere to investigate the kinetics of thermal degradation.

RESULTS AND DISCUSSION

Tensile Results Analysis

Tensile properties of PMVS/SiO_2/GO-C_{12}-hep nanocomposites with different content of GO-C_{12}-heparin filler are listed in Table I. Test results show that the tensile property of PMVS/SiO_2 sample obviously increase when it is filled with GO-C_{12}-hep filler. It can be attributed to nanofiller which act as the centers of crosslink and improve the tensile property of the nanocomposites.[25] From Table I, retained tensile test shows that tensile strength of PMVS/SiO_2/GO-C_{12}-hep nanocomposites increase with increasing the GO-C_{12}-hep content from 0 to 0.5 wt %, but it decreases when the GO-C_{12}-hep content is up to 0.8 wt %. So we can see that the sample of PMVS/SiO_2 filled with 0.5 wt % GO-C_{12}-hep has the best tensile property.

The scanning electron microscope (SEM) photo of PMVS/SiO_2 filled with 0.5 wt % GO-C_{12}-hep is shown in Figure 1.

It indicates that the GO-C_{12}-hep has been dispersed into PMVS matrix and the interfacial consistency property between GO-C_{12}-hep and PMVS is very good. This result manifested why PMVS/SiO_2/GO-C_{12}-hep nanocomposites have the superior tensile property.

ATR-FTIR Results Analysis

Indirect observation by ATR-FTIR was then necessary to characterize degradation of the silicone. Figure 2 presents the ATR-FTIR spectrum of degradation of PMVS/SiO_2/GO-C_{12}-hep and PMVS/SiO_2/GO-C_{12}-hep. The peaks at 1261 cm^{-1}, 1457 cm^{-1}, 1713 cm^{-1}, 2960 cm^{-1} are respectively attributed to C—H (bending vibration absorption peak of C—H in Si—CH_3), C—H (bending vibration absorption peak), C=O, C—H (stretching vibration absorption peak) in PMVS/SiO_2/GO-C_{12}-hep, but as we all know there are no peaks in the degradation of PMVS/SiO_2/GO-C_{12}-hep. It indicated that degradation of PMVS/SiO_2/GO-C_{12}-hep. In addition, the peaks at 798 cm^{-1} (Si—O—Si), 1103 cm^{-1} (SiO) are detected both for two samples, indicating that degradation of the silicone have the composition of SiO_2.

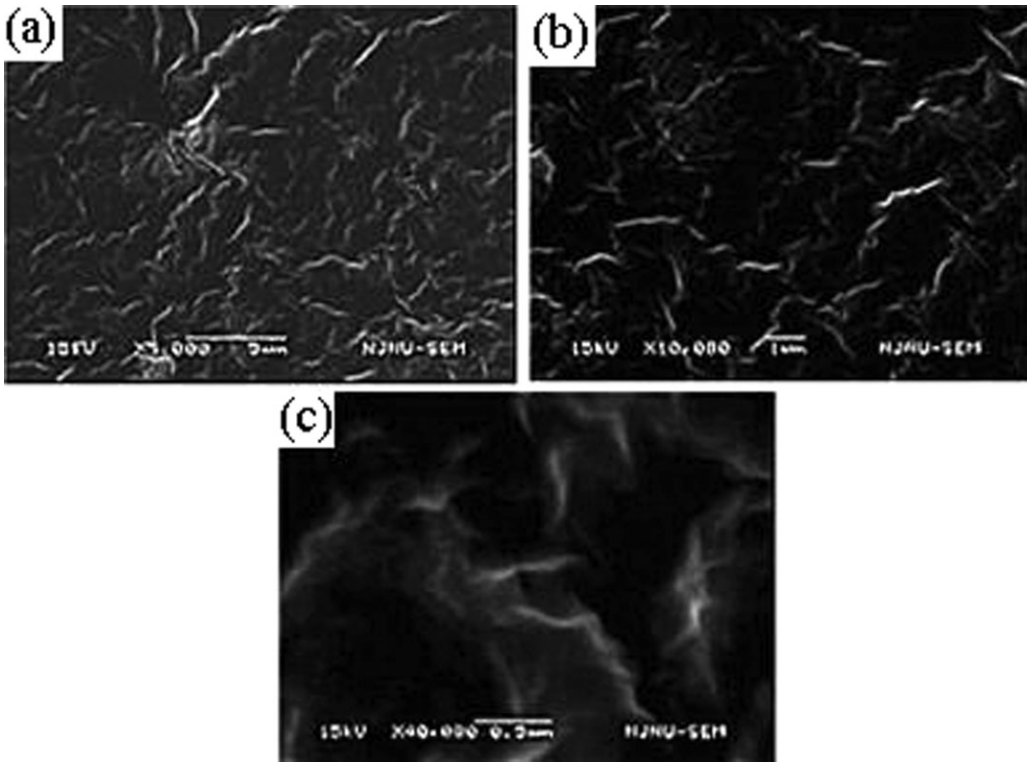

Figure 1. SEM photograph of PMVS/SiO_2/GO-C_{12}-hep nanocomposite: (a) 5000×, (b) 10,000×, (c) 40,000×.

TGA Results Analysis

TGA was employed in this research to determine the effect of the dispersion of GO-C12-hep into PMWS/SiO_2 matrix on the overall thermal stability of the elastomeric matrix. Figure 2 is a complex plot of the TGA mass loss curves for PMWS/SiO_2/GO-C12-hep nanocomposites containing 0, 0.2, 0.5, and 0.8 wt % of GO-C12-hep, respectively. From the mass loss curves it can be seen that all the samples show a single stage of degradation. PMWS/SiO_2 begins to decompose at about 435°C, while the presence of GO-C12-hep causes a shift of the initial mass loss toward higher temperatures. The TGA characteristic temperatures of the four kinds of nanocomposites are summarized in Table II. It shows that the mass loss in the sample of PMVS/SiO_2 occur between 435 and 582°C and those of PMVS/SiO_2/GO-C12-hep nanocomposites happen between 453 and 623°C. This indicates that the addition of GO-C12-hep is able to enhance the decomposition temperature of PMVS/SiO_2. Moreover, in the case of nanocomposites with the contents of GO-C12-hep from 0.2 wt % to 0.8 wt %, it is found that the decomposition temperatures increase with increasing the content of GO-C12-hep. It is mainly because of the following reasons: Firstly, nanolayer filler of GO can act as the centers of crosslink and improve the heat resistance of the PMVS/SiO_2/GO-C12-hep nanocomposites. The more content of nanolayer filler mean the more crosslink centers and the higher thermal degradation temperature.[26,27] Secondly, nanolayered structure of GO can reduce the thermal conductivity of the PMVS matrix. The more nanolayer structure of GO can result in the lower thermal conductivity of material.[28–30] Lastly, GO can adsorb

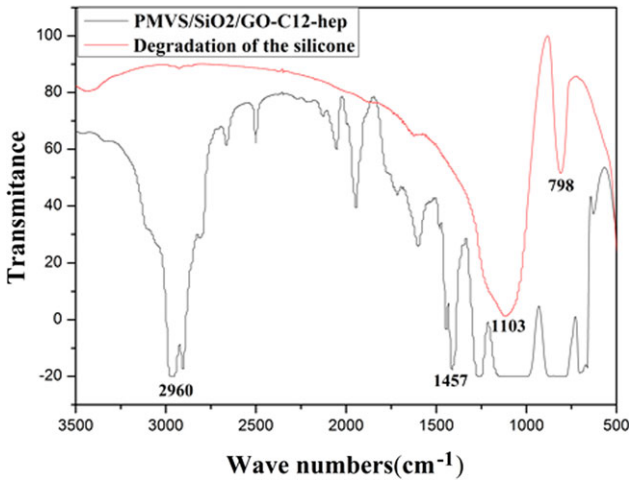

Figure 2. FTIR of PMVS/SiO_2/GO-C_{12}-hep nanocomposite and degradation of the PMVS/SiO_2/GO-C_{12}-hep. [Color figure can be viewed in the online issue, which is available at wileyonlinelibrary.com.]

Table II. Characteristic Thermal Decomposition Temperatures of PMVS/SiO_2/GO-$C1_2$-hep Nanocomposites

Sample	T_{onset} (°C)	T_{max} (°C)
PMVS/SiO_2	435.44	582.46
PMVS/SiO_2/GO-C12-hep-0.2%	453.49	594.65
PMVS/SiO_2/GO-C 12-hep-0.5%	462.52	611.69
PMVS/SiO_2/GO-C 12-hep-0.8%	479.06	623.75

Applied Polymer SCIENCE

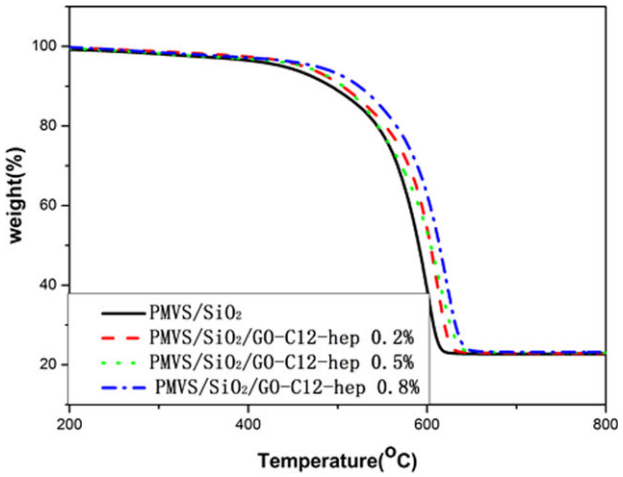

Figure 3. TGA curves of PMVS/SiO_2/GO-C_{12}-hep nanocomposites. [Color figure can be viewed in the online issue, which is available at wileyonlinelibrary.com.]

free radicals which are produced by thermal degradation and thus reduce the rate of chain reaction.[31,32]

Kinetics of Non-Isothermal Degradation

In this research, the E_a of the thermal degradation process of nanocomposites are determined by using Flynn–Wall–Ozawa method (FWO method) for dynamic heating experiment. FWO method can be employed to quantify E_a without any knowledge of the reaction mechanisms.

To TGA experimental data with a kinetic expression, a dimensionless mass loss has been defined as equation:

$$\alpha = \frac{M_0 - M}{M_0 - M_f} \tag{1}$$

where M, M_0, M_f are the actual, initial, and final sample weights. For non-isothermal degradation, M_0 is the mass at the start of the degradation process, and M_f is the steady state mass at the end of degradation. The term of $(M_0 - M_f)$ represents that the total mass of polymer is available for reaction.

The approximate FWO method can be shown as equation:

$$\log \Phi = \log AE/RF(\alpha) - 2.315 - 0.4567E/RT \tag{2}$$

where Φ is the heating rate of TGA, A is the pre-exponential factor, R is the universal gas constant, T is an absolute temperature, α is a dimensionless mass loss, and E is the activation energy of thermal decomposition.

Therefore, for α = const., the plot $\log \Phi$ vs. $1/T$, obtained from TGA recorded at a series of heating rates, should be a straight line whose slope allows evaluation of the thermal degradation activation energy (E_a). The TGA curves corresponding to the thermal degradation of PMVS/SiO_2 and PMVS/SiO_2/GO-C_{12}-hep nanocomposites at the heating rates: 5, 10, 20, 40°C /min are shown in Figure 3, and their plot $\log \Phi$ vs. $1/T$ are shown in Figure 4.

It can be clearly observed from Figure 3 that the mass loss curves of all samples at different heating rates show a shift of the degradation area to higher temperatures with the increase of heating rates; at the end of the degradation almost 25% residue remained. The relationship between kinetic parameters and conversion (α) can be found by using the mass loss curves recorded in TG dynamic curves. Figure 4 shows that the fitting straight lines are nearly parallel, which is an indication that the activation energies at different α are almost similar. Using FWO method, the E_a values and error corresponding to PMVS/SiO_2/GO-C_{12}-hep nanocomposites are listed in Figures 5 and 6. From it, we can see that the thermal degradation activation energy of composite filled with 0.5 wt % of GO-C_{12}-hep is obviously higher than those of the others, which correspond to the better tensile property.

As usual, the higher E_a value usually can be corresponding to the better thermal aging resistance and higher thermal degradation temperature. Therefore, the E_a results suggested that PMVS/SiO_2/GO-C_{12}-hep-0.5 wt % should have the highest thermal degradation temperature of all nanocomposites, which is not consistent with Table II.

It is well known that the molecular backbone of PMVS contain alternating units of silicon atoms and oxygen atoms (Si—O—Si—O). Its side chain is usually formed by methyl and sometimes they might contain a small amount of vinyl. The degradation mechanisms of silicone rubber mainly include the unzipped degradation [unzipping by catalyst participation, as Scheme 1, the random rearranged degradation along the main chain [molecular mechanisms, as Scheme 2 and the thermal oxidative degradation as Scheme 3. The unzipped degradation occurred mainly in the hydroxyl end-group containing silicone rubber. And the thermal degradation of —Si—$(CH_3)_3$ end-capped silicone rubber is almost attributed to the random rearranged degradation along the main chain. If O_2, H_2O, or other oxidative impurities exist in the silicone rubber composites, the thermal degradation will occur.

1. Unzipped degradation [Scheme 1]

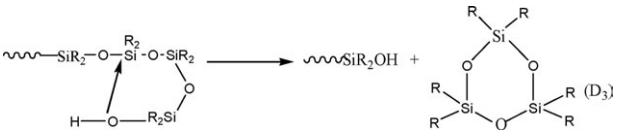

2. Random rearranged degradation along the main chain [Scheme 2]

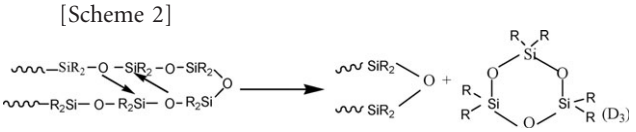

3. Thermo-oxidative degradation [Scheme 3][33]

$$\equiv SiCH_3 + O_2 \longrightarrow \equiv SiCH_2OOH \longrightarrow \equiv Si + CH_2OH_2 + OH$$
$$\equiv Si\bullet + OH\bullet \longrightarrow \equiv SiOH_2$$
$$\equiv SiOH \longrightarrow \equiv SiOSi\equiv + H_2O$$
$$CH_2O \longrightarrow CO + H_2$$
$$CH_2O + \longrightarrow CO_2 + H_2O$$

The reaction order n can be obtained by the Coatse Redfern method as the following relations and then linear fitting of the

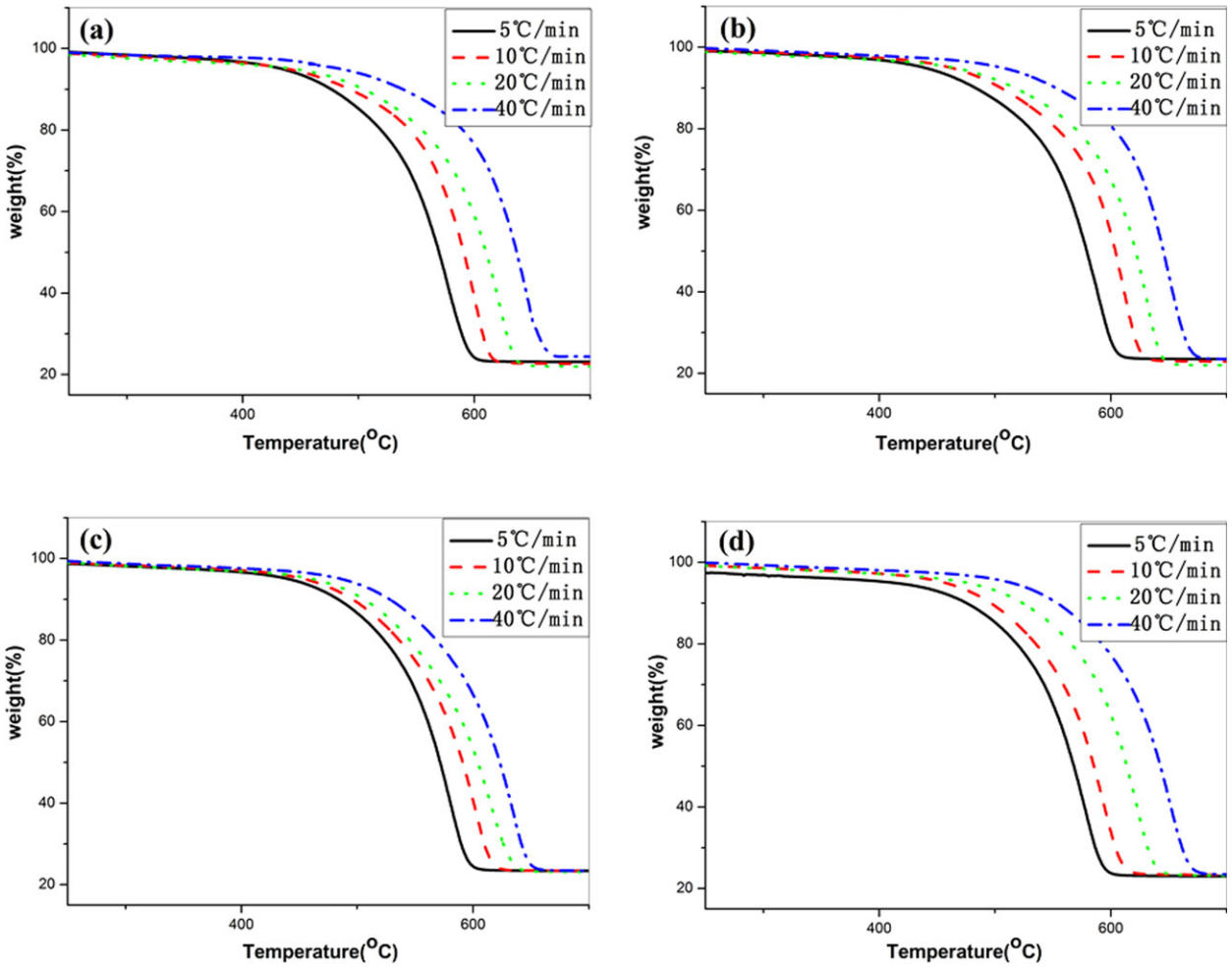

Figure 4. TGA curves of PMVS/SiO_2/GO-C_{12}-hep nanocomposites at the heating rates of 5, 10, 20, 40 °C/min: (a) PMVS/SiO_2, (b) PMVS/SiO_2/GO-C_{12}-hep-0.2%, (c) PMVS/SiO_2/GO-C_{12}-hep-0.5%, (d) PMVS/SiO_2/GO-C_{12}-hep-0.8%. [Color figure can be viewed in the online issue, which is available at wileyonlinelibrary.com.]

part of the equations' dependence of $1/T$ which are summarized in Figure 7, when the logarithmic term on the right part of the above equations is regarded as constant.[34]

$$n = 1 \quad \ln\left(-\frac{\ln(1-\alpha)}{T^2}\right) = \ln\left[\frac{AR}{\beta E_a}\left(-\frac{2RT}{E_a}\right)\right] - \frac{E_a}{RT} \tag{3}$$

$$n \neq 1 \quad \ln\left[-\frac{1-(1-\alpha)^{1-n}}{T^2(1-n)}\right] = \ln\left[\frac{AR}{\beta E_a}\left(-\frac{2RT}{E_a}\right)\right] - \frac{E_a}{RT} \tag{4}$$

E_a: apparent activation energies (kJ/mol^{-1}), A: pre-exponential factor (min)

n: apparent reaction order, R: gas constant (8.3136 J mol^{-1} K^{-1}), T: absolute temperature (K), α: conversion degree or fractional weight loss, t: reaction time (s), k: rate constant associated with the temperature.

The n value at the best correlation coefficient (R) is the real reaction order, and the fitted results including reaction order of the involved materials at various heating rates are summarized in Table III.

When the differential TG data of all samples at various heating rate (5, 10, 20, and 40°C/min) are plotted as indicated by Figure 7, straight-line plots were obtained in each case. So all samples reaction order is about 1.[35]

Thermal degradation mechanism of end-blocked with $(CH_3)_3Si$-groups polysiloxane can be considered as silicon atoms utilizing its vacant 3d-orbital to form energetically favorable dπ–pπ transition states with orbits of oxygen atom, and thus leading to siloxane backbone rearrange and produce cyclic oligomers. As PMVS/SiO_2 contains only polysilane linkages, the decomposition at 582°C is attributed to the degradation of these linkages. Linear polysilanes normally degrade at a low temperature, the higher T_{max} for PMVS/SiO_2/GO-C_{12}-hep is due to the presence of extensive crosslinks resulting from the participation of the vinyl group in the preparation. Therefore, the higher decomposition temperature for PMVS/SiO_2/GO-C_{12}-hep nanocomposites when compared to that of PMVS/SiO_2 is understood in view of the higher extent of crosslinking present in the case of the former and thus hinders the degradation of siloxane chains caused by heat rearrangement to a certain extent. It is

Applied Polymer SCIENCE

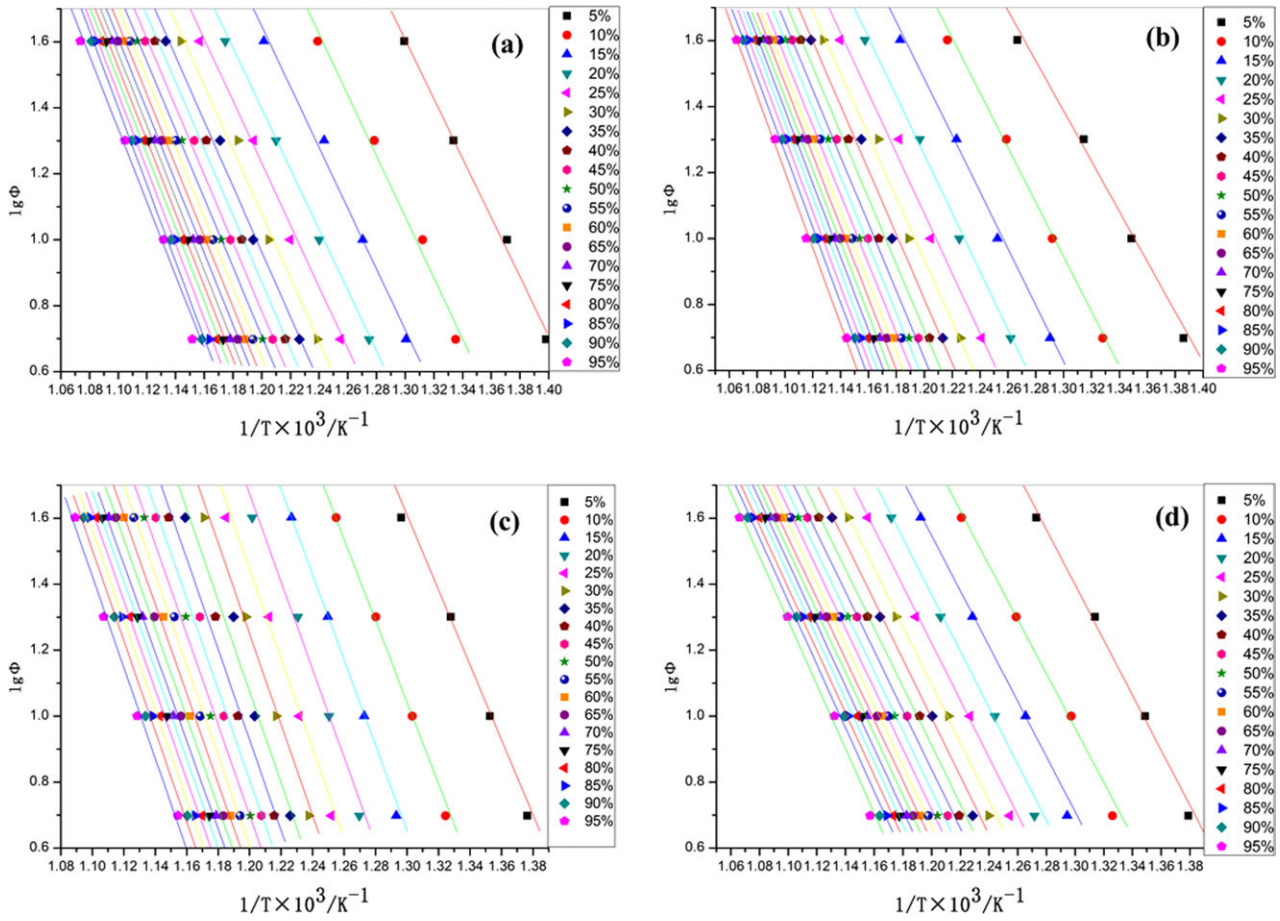

Figure 5. OFW plots for different degrees of conversion α, from α = 5% to α = 95% of PMVS/SiO_2/GO-C_{12}-hep nanocomposites: (a) PMVS/SiO_2, (b) PMVS/SiO_2/GO-C_{12}-hep-0.2%, (c) PMVS/SiO_2/GO-C_{12}-hep-0.5%, (d) PMVS/SiO_2/GO-C_{12}-hep-0.8%. [Color figure can be viewed in the online issue, which is available at wileyonlinelibrary.com.]

also observed that the decomposition temperature increase with increasing GO-C_{12}-hep content from 0 to 0.8 wt%. However, E_a of PMVS/SiO_2/GO-C_{12}-hep nanocomposites increase with increasing GO-C_{12}-hep content from 0 to 0.5 wt %, but it decreases when the GO-C_{12}-hep content is up to 0.8 wt %. Rings of low molecular cyclosiloxane were easily formed by short siloxane chains and Si—O chains because of the excess high crosslinking. It is observed that the decomposition temperature decline with increasing the GO-C_{12}-hep content from 0.5 wt % to 0.8 wt %.

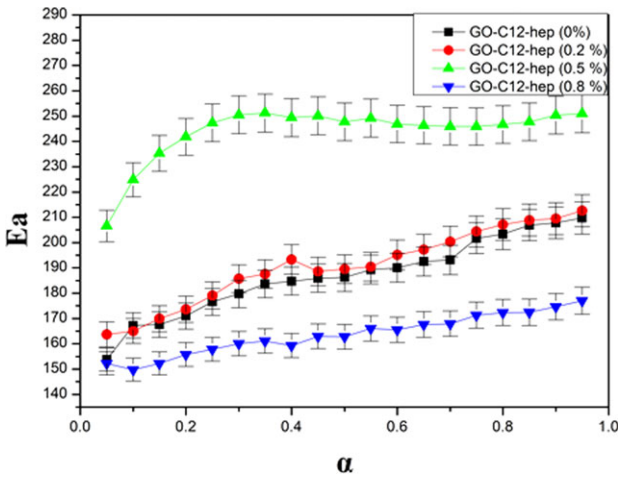

Figure 6. Activation energy and error for the thermal degradation of PMVS/SiO_2/GO/C_{12}-hep nanocomposites. [Color figure can be viewed in the online issue, which is available at wileyonlinelibrary.com.]

Under normal circumstances, the thermo degradation mode appears at lower temperatures. In the PMVS/SiO_2/GO-C_{12}-hep nanocomposites system, nanolayered structure of GO improves the stability of the system, which causes the higher thermo-oxidative degradation temperature and higher E_a. On the other hand, the carbonyl on the surface of GO can act as the oxidative impurities and promotes the thermo-oxidative degradation of PMVS, which cause the lower E_a of the system. Therefore, it can be considered that the competition of two factors above result in PMVS/SiO_2 filled with 0.8 wt % GO-C_{12}-hep having the higher degradation temperature and lower E_a than others.

CONCLUSIONS

In summary, we have synthesized a series of the PMVS/SiO_2/GO-C12-hep nanocomposites. The mechanical properties and the thermal decomposition temperature of PMVS/SiO_2/GO-

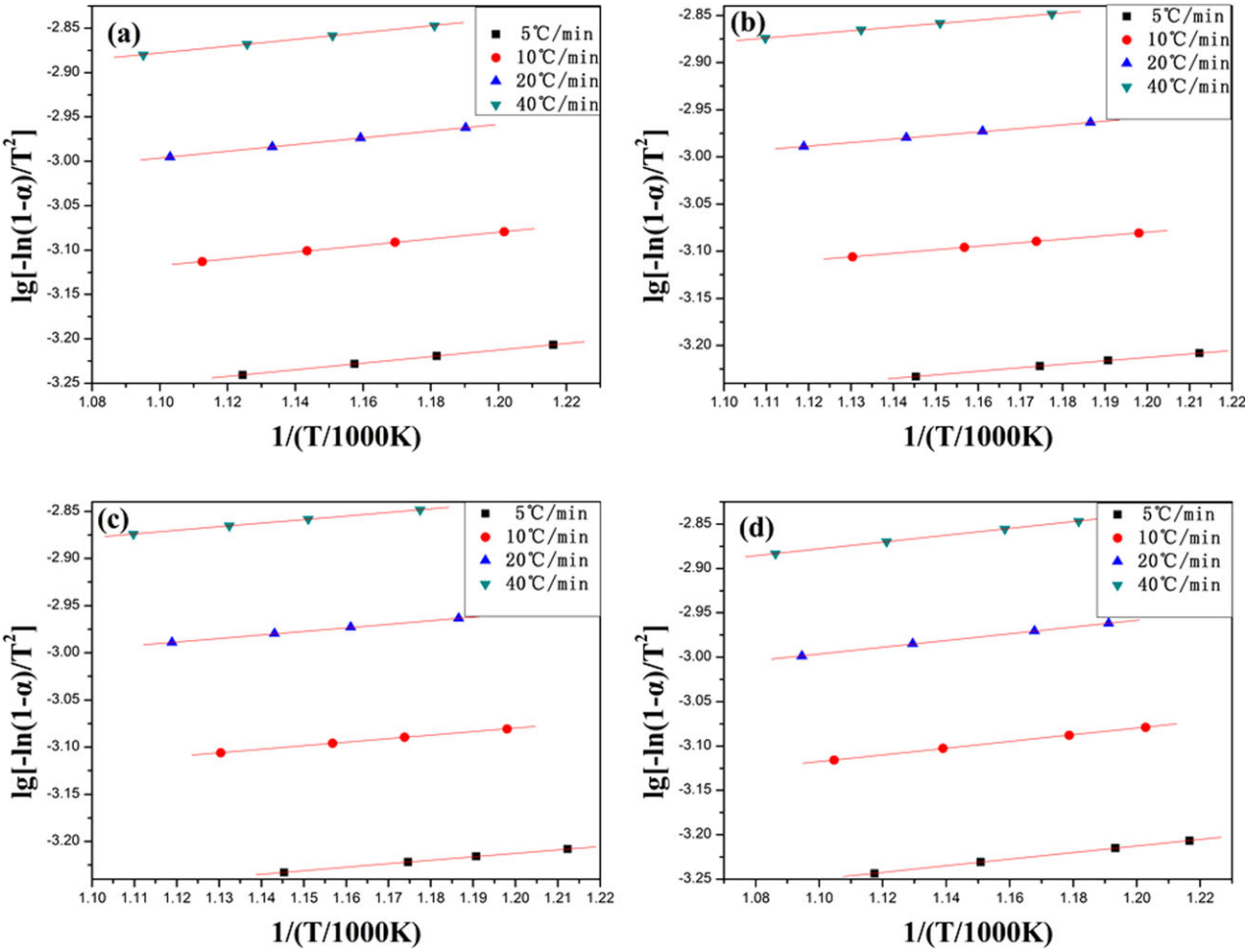

Figure 7. The reaction order *n* for the thermal degradation of PMVS/SiO_2/GO/C_{12}-hep nanocomposites using Coatse Redfern method. [Color figure can be viewed in the online issue, which is available at wileyonlinelibrary.com.]

Table III. Correlation Coefficient (R) of Different Samples Obtained Using CoatseRedfern Method at Different Heating Rates: (a) PMVS/SiO2, (b) PMV S/SiO2/GO-C12-hep-0.2%, (c) PDMS/SiO2/GO-C12-hep-0.5%, (d) PDMS/SiO2/GO-C12-hep-0.8%

Heating rate (β, °C/min)	Samples	Correlation coefficient (R)
5	PMVS/SiO_2	0.99992246
	PMV S/SiO_2/GO-C12-hep-0.2%	0.99991614
	PDMS/SiO_2/GO-C12-hep-0.5%	0.99995917
	PDMS/SiO_2/GO-C12-hep-0.8%	0.99993629
10	PMVS/SiO_2	0.99992814
	PMV S/SiO_2/GO-C12-hep-0.2%	0.99992355
	PDMS/SiO_2/GO-C12-hep-0.5%	0.99995665
	PDMS/SiO_2/GO-C12-hep-0.8%	0.99993269
20	PMVS/SiO_2	0.999931
	PMV S/SiO_2/GO-C12-hep-0.2%	0.99992853
	PDMS/SiO_2/GO-C12-hep-0.5%	0.99995653
	PDMS/SiO_2/GO-C12-hep-0.8%	0.99993238
40	PMVS/SiO_2	0.99993132
	PMV S/SiO_2/GO-C12-hep-0.2%	0.99993277
	PDMS/SiO_2/GO-C12-hep-0.5%	0.9999568
	PDMS/SiO_2/GO-C12-hep-0.8%	0.99993206

C12-hep are obviously improved in comparison with PMVS/SiO_2. When the PMVS/SiO_2 was filled with 0.5 wt % GO-C12-hep, the tensile strength values and the thermal degradation activation energy of all samples were highest in our experiment. And its bio-application will be investigated and researched in our future experiments.

ACKNOWLEDGMENTS

The project was supported by the National Natural Science Foundation of China (20874047), Natural Science Foundation of Jiangsu Province (BK2009408), the Perspective Research Foundation of Production Study and Research Alliance of Jiangsu Province of China (BY2011109) and the Priority Academic Program Development of Jiangsu Higher Education Institutions (PAPD).

REFERENCES

1. Diao, S.; Jin, K K.; Yang, Z. Z. *Mater. Chem. Phys.* **2011**, *129*, 202.
2. Kulik, V. M.; Boiko, A. V.; Bardakhanov, S. P. *Mater. Sci. Eng. A* **2011**, *528*, 5729.
3. Xu, Q.; Pang, M. L.; Zhu, L. X. *Mater Design.* **2010**, *31*, 4083.
4. Zhang, W. L.; Wu, Q.; Xu, G. Z. *Polym. Bull.* **2005**, *3*, 96.
5. Rodrigues, L. R.; Banat, I. M.; Teixeira, J. A.; Oliveira, R. *J. Appl. Microbiol.* **2006**, *100*, 470.
6. Julio, C. A.; Dequeiroz, A. A. A.; Higa, O. Z. *Braz. J. Med. Biol. Res.* **1994**, *11*, 2565.
7. Williams, R. L.; Wilson, D. J.; Rhodes, N. P. *Biomaterials* **2004**, *19*, 4659.
8. Zhou, J.; Yuan, X. P.; Zang, J. *J. Colloid Surf. B* **2005**, *1*, 55.
9. Tu, M.; Cha, Z. G.; Zhao, J. H.; Feng, B. H. *IET Nanobiotechnol.* **2007**, *6*, 87.
10. Chen, X. F.; Chen, G. H.; Wu, D. J.; Xu, J. R. *Polym. Bull.* **2004**, *4*, 39.
11. Han, Y. Q.; Lu, Y. *Carbon* **2007**, *45*, 2394.
12. Kaczmarek, H.; Podgórski, A. *Polym. Degrad. Stab.* **2007**, *92*, 939.
13. Holmstrom, N.; Askendal, A.; Tengvall, P. *Colloid Surf. B Biointerfaces* **1998**, *11*, 265.
14. Chen, J. Y.; Wang, L. P.; Fu, K. Y. *Surf. Coat. Technol.* **2002**, *156*, 289.
15. Li, G.; Liao, J. M.; Hu, G. Q. *Biosens. Bioelectron.* **2005**, *20*, 2140.
16. Szabo, T.; Szeri, A.; Dekany, I. *Carbon* **2005**, *43*, 87.
17. Wang, Z. M.; Hoshinoo, K.; Xue, M.; Kanoh, H. *Chem. Commun.* **2002**, 1696.
18. Kovtyukhova, N. I.; Ollivier, P. J.; Martin, B. R.; Mallouk, T. E.; Chizhik, S. A.; Buzaneva, E. V. *Chem. Mater.* **1999**, *11*, 771.
19. Murugesan, S.; Xie, J.; Linhardt, R. *J. Curr. Top. Med. Chem.* **2008**, *8*, 80.
20. Larsson, R. *Encyclopedia Biomater. Biomed. Eng.* **2004**, *1*, 753.
21. Keuren, J. F. W.; Wielders, S. J. H.; Willems, G. M.; Cahalan, M. L.; Cahalan, P. *Biomaterials* **2003**, *24*, 1917.
22. Tepe, G.; Schmehl, J. P.; Wendel, H.; Schaffner, S.; Heller, S.; Gianotti, M. *Biomaterials* **2006**, *27*, 643.
23. Thorsteinsson, T.; Loftsson, T.; Masson, M. *Soft Antibacter. Agents Curr. Med. Chem.* **2003**, *10*, 1129.
24. Zhou, N. L.; Meng, N.; Ma, Y. C. *Carbon* **2009**, *47*, 1343.
25. Yang, J. T.; Wu, M. J.; Chen, F. *J. Supercrit. Fluid.* **2011**, *56*, 201.
26. Jeong, H.-K.; Lee, Y. P.; Rob, J. W. E. L.. *JACS* **2008**, *130*, 1362.
27. Dreyer, D. R.; Park, S.; Bielawski, C. W. *CSR* **2009**, *10*, 1039.
28. Lee, D. W.; De Los Santos, L.; Seo, J. W. *J. Phys. Chem. B* **2010**, *114*, 5723.
29. Jeong, H.-K.; Lee, Y. P.; Jin, M. H. *Chem. Phys. Lett.* **2009**, *470*, 255.
30. Schniepp, H. C.; Li, J.-L.; McAllister, M. J. *JPC* **2006**, *110*, 8535.
31. Erickson, K.; Erni, R.; Lee, Z. *Adv. Mater* **2010**, *22*, 4467.
32. Tang, X.-Z.; Li, W.; Yu, Z.-Z. *Carbon* **2011**, *49*, 1258.
33. Lewis, C. W. *J. Polym. Sci.* **1959**, *37*, 425.
34. Chen, Y.; Wang, Q. *Polym. Degrad. Stab.* **2007**, *92*, 280.
35. Ozawa T *J. Therm. Anal.* **1970**, *2*, 301.